Electrical property effect of oxygen vacancies in the heterojunction of $LaGaO_3/SrTiO_3$*

Fu-Ning Wang(王芙凝), Ji-Chao Li(李吉超)†, Xin-Miao Zhang(张鑫淼), Han-Zhang Liu(刘汉璋), Jian Liu(刘剑), Chun-Lei Wang(王春雷), Ming-Lei Zhao(赵明磊), Wen-Bin Su(苏文斌), and Liang-Mo Mei(梅良模)

School of Physics, Shandong University, Jinan 250100, *China*

(Received 10 November 2016; revised manuscript received 27 December 2016; published online 13 February 2017)

Density functional theory within the local density approximation is used to investigate the effect of the oxygen vacancy on the $LaGaO_3/SrTiO_3$ (001) heterojunction. It is found that the energy favorable configuration is the oxygen vacancy located at the 3rd layer of the STO substrate, and the antiferrodistortive distortion is induced by the oxygen vacancy introduced on the $SrTiO_3$ side. Compared with the heterojunction without introducing oxygen vacancy, the heterojunction with introducing the oxygen vacancy does not change the origin of the two-dimensional electron gas (2DEG), that is, the 2DEG still originates from the d_{xy} electrons, which are split from the t_{2g} states of Ti atom at interface; however the oxygen vacancy is not beneficial to the confinement of the 2DEG. The extra electrons caused by the oxygen vacancy dominantly occupy the $3d_{x^2-y^2}$ orbitals of the Ti atom nearest to the oxygen vacancy, thus the density of carrier is enhanced by one order of magnitude due to the introduction of oxygen vacancy compared with the density of the ideal structure heterojunction.

Keywords: two-dimensional electron gas (2DEG), first-principles calculation, oxygen vacancy

PACS: 71.10.Ca, 63.20.dk, 61.72.jd **DOI:** 10.1088/1674-1056/26/3/037101

1. Introduction

In the last decades, heterostructures based on perovskite transition metal oxides have attracted much attention, particularly due to the discoveries of extraordinary electronic and magnetic properties of the internal interface. For example, the two-dimensional electron gas (2DEG) with high mobility was observed at the interface between $LaAlO_3$ (LAO) and $SrTiO_3$ (STO), which exhibit insulating electrical properties in bulk materials.[1,2] Since then, some novel physical properties have been observed at the interface of oxide heterojunction, such as magnetism,[3] superconductivity[4,5] and the coexistence of magnetism and superconductivity.[6–8] The mechanism of the 2DEG formed at the interface between insulated oxides has been widely investigated both in theory[9–15] and experiments.[16–20] Especially, the heterostructures of $LaGaO_3$ (LGO) and STO have received more and more attention due to their two-dimensional electrical properties at interface.[21–26]

In 2010, Perna *et al.*[21] first observed the 2DEG formed at the interface of LGO/STO, which exhibits some properties similar to those of LAO/STO, such as superconducting at low temperature ($T_c = 150$ mK for both heterostructures). The onset of conductivity takes place at 4 unit cells (u.c.) for both LAO/STO[2] and LGO/STO[21] interface. With using the electronic reconstruction model, our previous calculations show that the origin of the 2DEG is partly filled d_{xy} orbital split from t_{2g} states of Ti atom of the interface caused by symmetry broken. Though the electronic reconstruction has performed to explain the mechanism of the 2DEG formed at ideal LAO/STO interface,[27,28] there are also abundant evidences that the creations of oxygen vacancies during the growth of the oxide heterostructures play an important role in determining the transport properties for the LAO/STO system.[2,16,17,29] Experimentally, Amoruso *et al.* found that the interface produced at an oxygen pressure of 10^{-1} mbar, at which the interface should be free from oxygen defects, did not show a 2DEG, unlike the conductive interface obtained in low oxygen pressure.[23] However, the experiments reported by Aruta *et al.* demonstrated a direct link between the target-to-substrate distance and the interface sheet resistance, that is to say, the insulating interface was caused by the increase of the target-to-substrate distance.[24] Anyway, the mechanism of the electrical property effect of the oxygen vacancy has not been fully understood. A better understanding of the effect of oxygen vacancies on interface electronic states of LGO/STO and the distribution character of the induced charge carriers is lacking.

In this article, the first-principles calculations are employed to investigate the LGO/STO n-type interface with and without oxygen vacancy (V_O). The values of formation energy of the V_O located at different layers of the STO substrate are calculated to find the most suitable configuration for stabilizing the system. Then, the role of the V_O in generating the 2DEG is explored and the electrical property effect of the V_O on the LGO/STO heterojunction is discussed.

*Project supported by the National Basic Research Program of China (Grant No. 2013CB632506) and the National Natural Science Foundation of China (Grant Nos. 11374186, 51231007, and 51202132).

†Corresponding author. E-mail: lijichao@sdu.edu.cn

© 2017 Chinese Physical Society and IOP Publishing Ltd

2. Models and computational details

We investigate an n-type LGO/STO supercell with a 2×1 surface unit cell consisting of 5 u.c. layers of STO substrate and 7 u.c. layers of LGO film along the (001) direction as shown in Fig. 1. The vacancy is introduced by excluding the oxygen atom O at the center of the Ti_2O_4-plaquette. To minimize the interaction between neighboring surfaces, the slabs are separated in the z-direction by 12 Å of vacuum. Considering that the LGO films are grown on the STO substrates, the in-plane lattice constants are all fixed at the bulk-STO cubic value ($a = 3.905$ Å). We also fix the bottom two layers of STO to simulate the real heterostructure films. Density functional calculations are performed by using the projector augmented wave method as implemented in the Vienna *ab initio* Simulation Package (VASP).[30] The electronic exchange correlation potential is parameterized in the local density approximate (LDA).[31] We do not include the Coulomb corrections within the local density approximation LDA$+U$ functional, as it may not describe the correlation effect properly for the low carrier density case.[9] The cut-off energy for plane wave basis set is chosen to be 400 eV. The supercell c axis is optimized by minimizing the total energy. Ionic relaxation along the z axis is performed until the forces acting on atoms were less than 0.01 eV/Å except for the atoms in the bottom two layers of STO which are fixed at the bulk positions, as mentioned before.

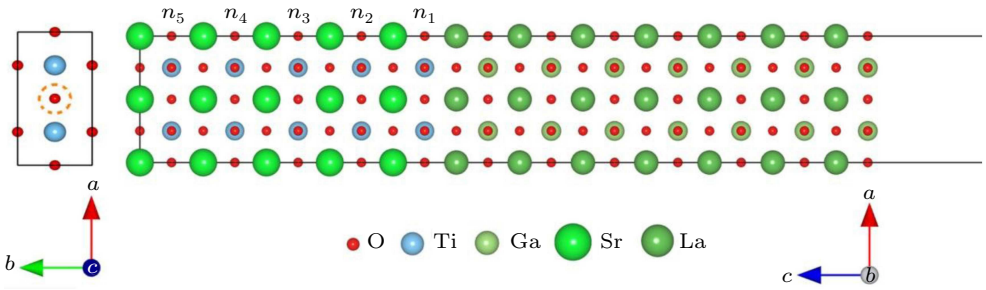


Fig. 1. (color online) Schematic illustration of the $(LGO)_7/(STO)_5$ slab with n-type interface. The left panel indicates the position of the V_O by the circle.

3. Results and discussion

In order to evaluate the stability of the defective system, the values of formation energy of the V_O at various positions are calculated. In this calculation, only the V_O located on STO side named by n_1–n_5 is investigated for the LGO/STO heterojunction, which is shown in Fig. 1. The formation energy of a single V_O in the STO overlayer is given by[32]

$$E_f = E_{def} - E_{bulk} + 1/2E(O_2),$$

where E_{def} is the calculated total energy of the supercell with one V_O and E_{bulk} is the total energy of the supercell without V_O. The $1/2E(O_2)$ is the chemical potential of an oxygen atom, which is obtained at the oxygen-rich limit.[33]

The values of formation energy of the V_O are calculated by DFT method, and shown in Fig. 2. This figure shows that the formation energy decreases monotonically from n_1 to n_3 and then rise from n_3 to n_4, from n_4 to n_5 there is a negligible decline. The formation energy reaches the maximum at the interface of the supercell. The value represents how easily a vacancy can be created. So it is more stable for the V_O located at the 3rd TiO_2 layer of the STO substrate. It should be noted that the variations of formation energy of V_O at different positions are independent of the oxygen chemical potential. The values presented in Fig. 2 are for O-rich growth condition and the ideal structure is always more stable than the defective one. However, under the O-poor condition, which corresponds to the low chemical potential of oxygen, the actual values of the formation energies can be much smaller. For V_O at the position located at the 3rd TiO_2layer, if the oxygen chemical potential is lower than a critical value of -5.09 eV, the formation energy will be negative, which means that the V_O can be spontaneously formed during the growth. In other words, the defective structure becomes more stable than the ideal one.[33] It has been experimentally discovered that at low oxygen pressure the oxygen can be easily removed from the STO substrate.[17] Our calculations are in agreement with the experimental results.

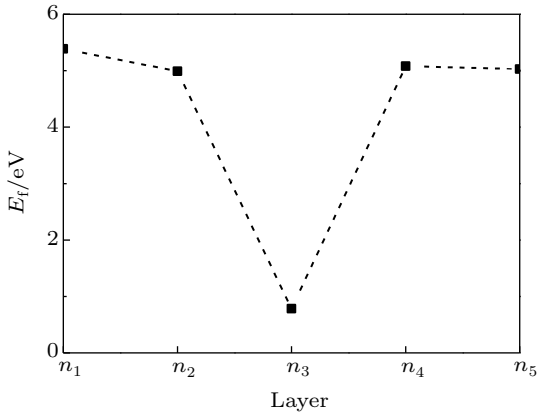


Fig. 2. The formation energy of the V_O in the STO overlayers. The designations of the layers are marked in Fig. 1.

In order to compare the effect of the relaxation, the atomic distortions which are exclusively along the *c*-axis for the bulk, i.e., the supercell without V_O and for the supercell with one V_O in the 3rd TiO_2 layer, are displayed in Fig. 3. The relative displacement between cations and anions (ΔZ) in each layer of the bulk is shown in Fig. 3(a). This figure shows that there is a strong buckling in each of all LaO layers of 0.18–0.27 Å and the largest relaxation appears at the LaO layer far from the interface. The surface GaO_2 layer shows a buckling of 0.07 Å, while the subsurface GaO_2 layers are buckled by about 0.14 Å. The Ti and O ions at the interface show a small buckling of 0.03 Å. Apparently the polar distortion in STO layer becomes extremely smaller than that in LGO layers. Our calculations fit well to previous calculation.[25]

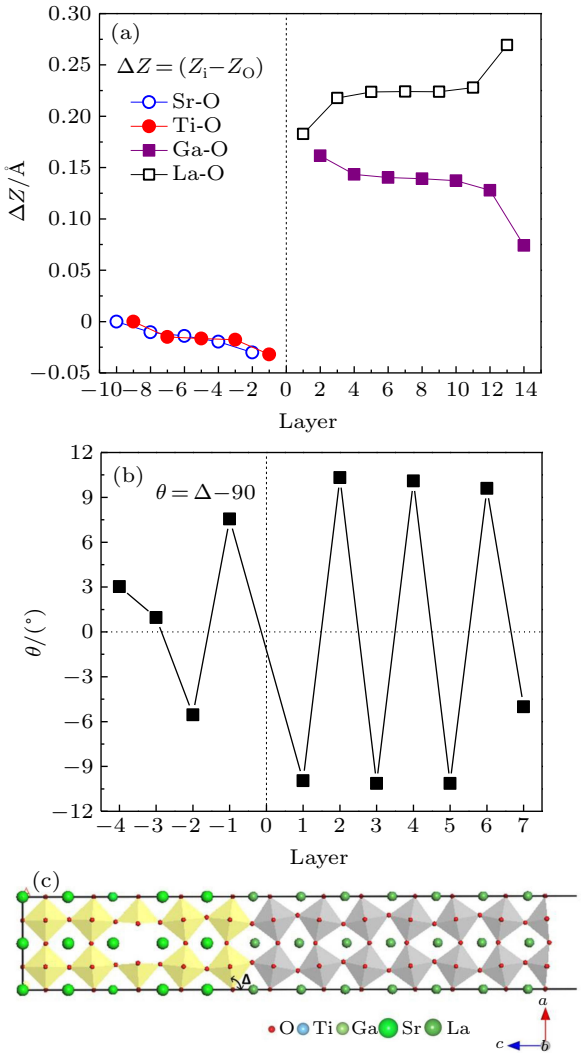


Fig. 3. (color online) (a) Relative displacements between the cations and the oxygen anions in each layer for the ideal $(LGO)_7/(STO)_5$ slab. (b) Rotation angle of the oxygen octahedron along the stacking direction for the defective $(LGO)_7/(STO)_5$ slab with one V_O in the 3rd layer of STO. (c) AFD distortions for the defective heterojunction.

For the supercell with one V_O in the 3rd layer, an unexpected pattern is discovered. Oxygen octahedron rotates oppositely in adjacent cells. The value of rotation angle is shown in Fig. 3(b). For the first GaO_6 octahedron near the interface the oxygen octahedral rotation angle is nearly 10° and with almost the same value the following octahedron rotates in the opposite direction. For Ga in the surface the oxygen octahedral rotation angle becomes smaller (5°). On the STO side, the rotations of TiO_6 octahedrons are not as striking as GaO_6 octahedrons. For the interfacial TiO_6 octahedron the rotation angle is 7° and for Ti in the 3rd layer the rotation angle is nearly 1°. Obviously the presence of a vacancy breaks the symmetry of the structure and causes the asymmetric oxygen octahedron to rotate. This kind of distortion is described as an antiferrodistortive (AFD) distortion, which is also discovered at the Cs/STO interface.[34]

In order to explore the effect of such an AFD distortion on the type of electronic states around the Fermi level and their spatial distribution, the density of states projected on the ten layers of LGO and STO for $(LGO)_7/(STO)_5$ with one V_O in the 3rd layer are obtained in our calculations, and shown in Fig. 4. A comparison between Fig. 4(a) with Fig. 4(b) shows that the conduction bands below Fermi surface occur only on the side of STO, and the side of LGO is insulated. For comparison, layer-projected density of states of STO for the defect-free system is also shown in Fig. 4(c). The figure shows that the 2DEG emerges mainly at the interface. By analyzing the density of states of STO near Fermi level, the total sheet carrier density is obtained to be $n_s = 7.23 \times 10^{13}$ cm^{-2}. This value is consistent with observations of high carrier density ($\sim 10^{13}$ cm^{-2}) in experiments of the LAO/STO heterostructure.[2,3,29,35] For the defective system, from the layer-by-layer density of states (DOS) on the STO side shown in Fig. 4(b), it can be clearly seen that charges are transferred throughout the entire STO film and not evenly distributed. The sheet carrier is increased by one order of magnitude, i.e., $n_s = 5.70 \times 10^{14}$ cm^{-2}. They are widely distributed throughout the substrate rather than localized only at the interface, which was also inferred from experiments.[17,29] Since a V_O adds two extra electrons in the system to preserve charge neutrality, the Bader charges on the Ti atoms in defect-free and defective system are calculated and the electron difference is listed in Table 1. Here we just show the electron difference of one Ti atom in each layer because the other one obtains the same number of electrons. As can be seen from the table, the Ti atom nearest to the V_O obtains far more electrons than the Ti atoms in other layers; meanwhile, the Ti atom at the interface obtains the least.

Table 1. Electron difference of one Ti atom in each layer between defective $(LGO)_7/(STO)_5$ and defect-free $(LGO)_7/(STO)_5$.

Ti	n_1	n_2	n_3	n_4	n_5
Electron difference /e	0.0112	0.0765	0.25	0.0665	0.0552

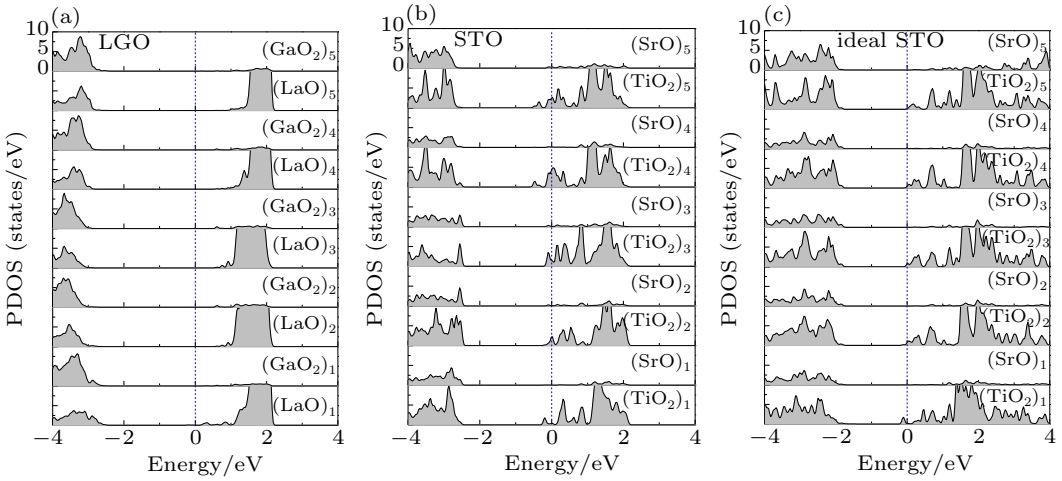


Fig. 4. (color online) Partial densities of states grouped by layers of (a) LGO and (b) STO for the defective $(LGO)_7/(STO)_5$ slab with one V_O in 3rd layer of STO and (c) STO for the ideal slab. The vertical dash line indicates the Fermi energy located at 0 eV.

In order to investigate the 2DEG effect of introducing the oxygen vacancy in the heterojunction, the orbital decomposed DOSs for the Ti atoms at the interface and in the 3rd layer are calculated, and the results are shown in Fig. 5. Figure 5(a) shows that the bands of the Ti 3d electrons states are near to the Fermi level, and the Ti t_{2g} electrons states split into the d_{xy} and d_{xz}/d_{yz} states, the in-plane d_{xy} orbital becomes the lowest conduction bands with low effective mass, so the contribution of the 2DEG comes from the partly filled d_{xy} orbitals of Ti atom of the interface. In our previous calculations,[26] the 2DEG of the ideal structure of the LGO/STO originates from the partly filled d_{xy} orbital split from t_{2g} states of Ti atoms at the interface caused by symmetry broken. Comparing our results with the previous ones, it is found that the introduction of the V_O does not change the origin of the 2DEG. In contrast, an unexpected pattern occurs for the Ti atom residing in the 3rd layer as illustrated in Fig. 5(b). The d_{xy} orbital is occupied slightly; meanwhile, the occupancies of the d_{xz} and d_{yz} orbitals are enhanced. Furthermore, the e_g states split into $d_{x^2-y^2}$ and d_{z^2} under the symmetry-reduced environment due to the presence of the V_O. Both of the $d_{x^2-y^2}$ and d_{z^2} orbitals are occupied and the $d_{x^2-y^2}$ state becomes occupied dominantly. Except for the Ti atoms nearest to the V_O, the lowest conduction band recovers its t_{2g} character (not shown). Here, it is also found that for two O atoms around Ti atom in the 3rd layer, the near Fermi energy states are also occupied by the O 2p orbitals, mainly the O $2p_x$ and $2p_y$ orbitals, though they only take a small proportion compared with the Ti 3d states. We assume that the hybridization between the Ti e_g and O 2p orbitals may be strong, which pushes the $d_{x^2-y^2}$ level down significantly. The extra electrons from the V_O, which are confined to the Ti 3d–e_g orbitals, may help to stabilize the oxygen-deficient system more effectively.

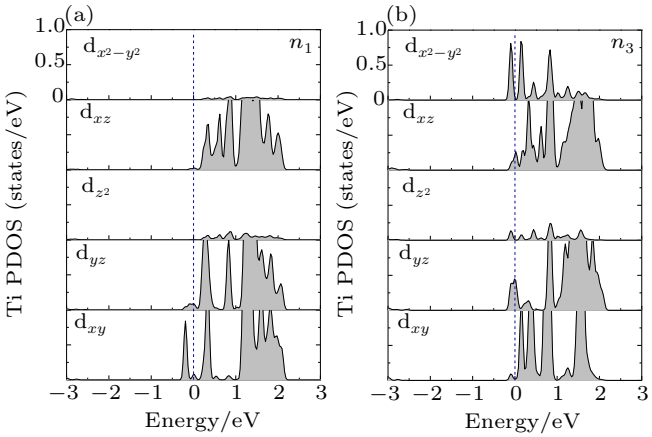


Fig. 5. The orbital decomposed DOSs for (a) the interfacial Ti atom and (b) the Ti atom nearest to the V_O in the 3rd layer of STO for the defective $(LGO)_7/(STO)_5$ heterojunction.

4. Conclusions

The local density approximation methods are employed to investigate the effect of the V_O on the LGO/STO heterojunction. Based on the values of formation energy of the V_O at the positions located at different layers, it is found that the energy favorable configuration is the V_O at the position located at the 3rd layer of the STO substrate, and the AFD distortion can be caused by the V_O. The introduction of the V_O does not change the origin of the 2DEG, namely the Ti d_{xy} electrons. However, the V_O is not beneficial to the confinement of the 2DEG. The density of the carriers is enhanced by the V_O by one order of magnitude compared with that of the ideal heterojunction. At the Ti nearest to the V_O, a strong e_g splitting happens and the $d_{x^2-y^2}$ state becomes occupied dominantly by the extra electrons from the V_O.

References

[1] Ohtomo A and Hwang H Y 2004 *Nature* **427** 423

[2] Thiel S, Hammerl G, Schmehl A, Schneider C W and Mannhart J 2006 *Science* **313** 1942

[3] Brinkman A, Huijben M, Van Zalk M, Huijben J, Zeitler U, Maan J C, Van der Wiel W G, Rijnders G, Blank D H A and Hilgenkamp H 2007 *Nat. Mater.* **6** 493

[4] Reyren N, Thiel S, Caviglia A D, Kourkoutis L F, Hammerl G, Richter C, Schneider C W, Kopp T, Ruetschi A S, Jaccard D, Gabay M, Muller D A, Triscone J M and Mannhart J 2007 *Science* **317** 1196

[5] Caviglia A D, Gariglio S, Reyren N, Jaccard D, Schneider T, Gabay M, Thiel S, Hammerl G, Mannhart J and Triscone J M 2008 *Nature* **456** 624

[6] Li L, Richter C, Mannhart J and Ashoori R C 2011 *Nat. Phys.* **7** 762

[7] Bert J A, Kalisky B, Bell C, Kim M, Hikita Y, Hwang H Y and Moler K A 2011 *Nat. Phys.* **7** 767

[8] Dikin D A, Mehta M, Bark C W, Folkman C M, Eom C B and Chandrasekhar V 2011 *Phys. Rev. Lett.* **107** 056802

[9] Popovic Z S, Satpathy S and Martin R M 2008 *Phys. Rev. Lett.* **101** 256801

[10] Pentcheva R and Pickett W E 2009 *Phys. Rev. Lett.* **102** 107602

[11] Li J C C, Beltran J I and Munoz M C 2013 *Phys. Rev. B* **87** 075411

[12] Ong P V and Lee J 2013 *Phys. Rev. B* **87** 195212

[13] Zhong Z C, Toth A and Held K 2013 *Phys. Rev. B* **87** 161102

[14] Du Y L, Wang C L, Li J C, Zhang X H, Wang F N, Liu J, Zhu Y H, Yin N and Mei L M 2015 *Chin. Phys. B* **24** 037301

[15] Du Y L, Wang C L, Li J C, Xu P P, Zhang X H, Liu J, Su W B and Mei L M 2014 *Chin. Phys. B* **23** 087302

[16] Herranz G, Basletic M, Bibes M, Carretero C, Tafra E, Jacquet E, Bouzehouane K, Deranlot C, Hamzic A, Broto J M, Barthelemy A and Fert A 2007 *Phys. Rev. Lett.* **98** 216803

[17] Kalabukhov A, Gunnarsson R, Borjesson J, Olsson E, Claeson T and Winkler D 2007 *Phys. Rev. B* **75** 121404

[18] Basletic M, Maurice J L, Carretero C, Herranz G, Copie O, Bibes M, Jacquet E, Bouzehouane K, Fusil S and Barthelemy A 2008 *Nat. Mater.* **7** 621

[19] Cen C, Thiel S, Mannhart J and Levy J 2009 *Science* **323** 1026

[20] Chen Y Z, Pryds N, Sun J R, Shen B G and Linderoth S 2013 *Chin. Phys. B* **22** 116803

[21] Perna P, Maccariello D, Radovic M, Scotti di Uccio U, Pallecchi I, Codda M, Marre D, Cantoni C, Gazquez J, Varela M, Pennycook S J and Miletto Granozio F 2010 *Appl. Phys. Lett.* **97** 152111

[22] Nazir S, Singh N and Schwingenschlogl U 2011 *Appl. Phys. Lett.* **98** 262104

[23] Amoruso S, Aruta C, Aurino P, Bruzzese R, Wang X, Granozio F M and di Uccio U S 2012 *Appl. Surf. Sci.* **258** 9116

[24] Aruta C, Amoruso S, Ausanio G, Bruzzese R, Di Gennaro E, Lanzano M, Granozio F M, Riaz M, Sambri A, di Uccio U S and Wang X 2012 *Appl. Phys. Lett.* **101** 031602

[25] Xu Q F, Wu D and Li A D 2013 *Phys. Lett. A* **377** 577

[26] Wang F, Li J, Du Y, Zhang X, Liu H, Liu J, Wang C and Mei L 2015 *Appl. Surf. Sci.* **355** 1316

[27] Nakagawa N, Hwang H Y and Muller D A 2006 *Nat. Mater.* **5** 204

[28] Pentcheva R and Pickett W E 2006 *Phys. Rev. B* **74** 035112

[29] Siemons W, Koster G, Yamamoto H, Harrison W A, Lucovsky G, Geballe T H, Blank D H A and Beasley M R 2007 *Phys. Rev. Lett.* **98** 196802

[30] Kresse G and Furthmuller J 1996 *Phys. Rev. B, Condens. Matter* **54** 11169

[31] Ceperley D M and Alder B J 1980 *Phys. Rev. Lett.* **45** 566

[32] Zhong Z C, Xu P X and Kelly P J 2010 *Phys. Rev. B* **82** 165127

[33] Li Y, Phattalung S N, Limpijumnong S, Kim J and Yu J 2011 *Phys. Rev. B* **84** 245307

[34] Jaekwang L, Chungwei L and Demkov A A 2013 *Phys. Rev. B* **87** 165103

[35] Chen Y Z, Pryds N, Kleibeuker J E, Koster G, Sun J R, Stamate E, Shen B G, Rijnders G and Linderoth S 2011 *Nano Lett.* **11** 3774